

15.2

## Controllable formation of TiO<sub>2</sub>–rutile nanostructures with a specified morphology using thermal oxidation technique

© S.A. Khubezhov<sup>1–3</sup>, E.Yu. Ponkratova<sup>2</sup>, M.E. Karsakova<sup>2</sup>, V.V. Prigodich<sup>4</sup>, O.I. Il'in<sup>1</sup>, I.V. Silaev<sup>3</sup>, I.V. Tvauri<sup>3</sup>, D.V. Yakimchuk<sup>4</sup>, E.Yu. Kaniukov<sup>5</sup>, D.A. Zuev<sup>2</sup>

<sup>1</sup> Institute of Nanotechnologies, Electronics and Equipment Engineering, Southern Federal University, Taganrog, Russia

<sup>2</sup> ITMO University, St. Petersburg, Russia

<sup>3</sup> Khetagurov North Ossetian State University, Vladikavkaz, Russia

<sup>4</sup> Scientific-Practical Materials Research Center of NAS of Belarus, Minsk, Belarus

<sup>5</sup> National University of Science and Technology MISiS, Moscow, Russia

E-mail: Soslan.khubezhov@gmail.com

Received March 9, 2022

Revised May 2, 2022

Accepted May 13, 2022

Titanium dioxide nanostructures are formed by a simple one-stage method of thermal oxidation of titanium in the temperature range of 700–900°C. The structures were studied by high-resolution electron microscopy and X-ray diffraction. It is shown that, depending on the temperature, nanostructures in the form of crystallites, granules, and dendrites of TiO<sub>2</sub>–rutile are formed on the surface of metallic titanium. The proposed method is promising for the large-scale creation of advanced functionalized TiO<sub>2</sub> surfaces applicable in catalysis and sensorics.

**Keywords:** nanostructures, titanium dioxide, thermal oxidation, morphology, dendrites.

DOI: 10.21883/TPL.2022.07.54031.19185n

Metal–oxide structures based on titanium dioxide attract close attention of researchers because they are promising for creating catalysts, gas sensors, plasmonic resonators, optical elements for solar energetics, etc. [1,2]. Development of new techniques and approaches for obtaining metal oxides with pre-specified parameters and properties is promoted by the possibility of creating based on them unique structures able to more efficiently convert the light energy and increase the effective reaction area. The application range wideness is caused by the TiO<sub>2</sub> nanostructure properties directly dependent on the morphology, structure and stoichiometry. For instance, catalytic activity and photoactivity of the TiO<sub>2</sub>–based systems depend on the phase composition of the anatase/rutile titanium oxide [3]. Nanostructured titanium dioxide of the rutile structural modification gets formed during titanium oxidation at the temperatures above 500°C [4].

Searching for simple approaches to creating TiO<sub>2</sub>–based nanomaterials is a crucial task of the up-to-date material research. Among the most common techniques, it is possible to distinguish the sol–gel method, anodization and reactive evaporation, or titanium heating in oxygen [5,6]. The advantages of the last technique are its simplicity, possibility of controlling the morphology, and relatively high rate of the process of obtaining the TiO<sub>2</sub>–based nanostructures, which significantly extends the technique application area.

In this work, the possibility of controllable fabrication of titanium dioxide nanostructures by the titanium thermal oxidation in oxygen–containing atmosphere was demonstrated

for the first time; the morphology and specific structural features of the obtained samples were studied in details.

Prior to the sample formation, titanium foil VT1-00 GOST 22178–76 50 × 10 × 0.08 mm in size was subjected to ion–plasma treatment in vacuum ( $4.2 \cdot 10^{-5}$  mbar). Titanium was oxidized by the method of thermal oxidation in oxygen–containing atmosphere at partial pressure  $P_{O_2} = 100$  mbar. The titanium foil was heated to the pre-specified temperature by passing electric current through it (direct electrical heating). The oxidation temperatures were  $T = 700, 800$  and  $900^\circ\text{C}$ , the time of exposure was  $t = 1.5$  min. After heating to  $T = 500^\circ\text{C}$  for  $t = 0.3$  min, the voltage and current were  $U = 4$  V and  $I = 25$  A, respectively. As the oxidation developed, the foil resistance changed; therefore, in order to ensure a uniform temperature increase, the current and voltage were dynamically varied in the automatic mode by feedback. Once the titanium oxides were formed, the films were annealed at  $T = 200^\circ\text{C}$  in high vacuum ( $4.2 \cdot 10^{-5}$  mbar) for  $t = 20$  min in order to reach thermodynamic equilibrium and remove hydroxyl groups; the total time of preparing the samples did not exceed 50 min. Morphology of the obtained structures was examined by scanning electron microscopy (SEM) using setup Nova NanoLab 600 (FEI, Netherlands) in the secondary electron mode. Structural analysis of the samples was performed by X-ray diffraction (XRD) using diffractometer XRD-7000 Maxima (Shimadzu) equipped with the characteristic X-ray source  $\text{CuK}_\alpha$  ( $\lambda = 0.15406$  nm). The data was recorded in the Bragg–Brentano geometry  $\theta$ – $2\theta$  with the angular speed of  $2^\circ/\text{min}$  and step of  $0.01^\circ$ .

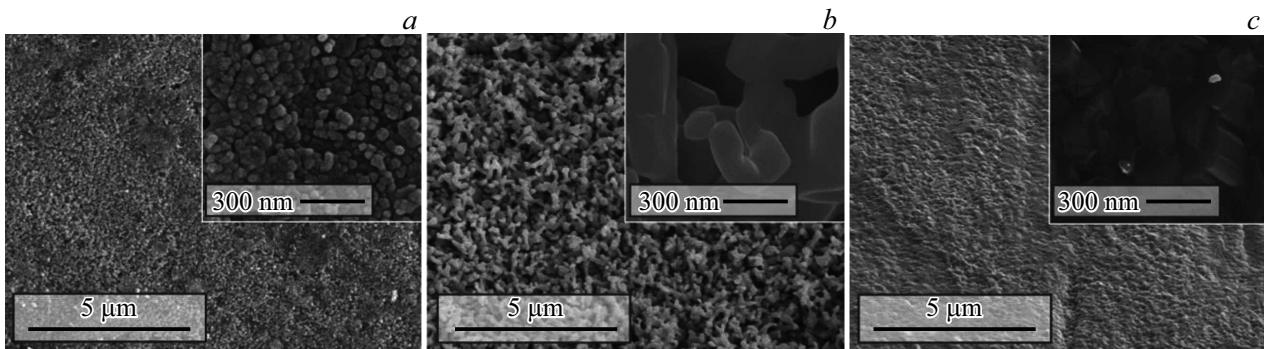


**Figure 1.** SEM images of the  $\text{TiO}_2$  samples obtained at  $T = 700$  (a),  $800$  (b) and  $900^\circ\text{C}$  (c).

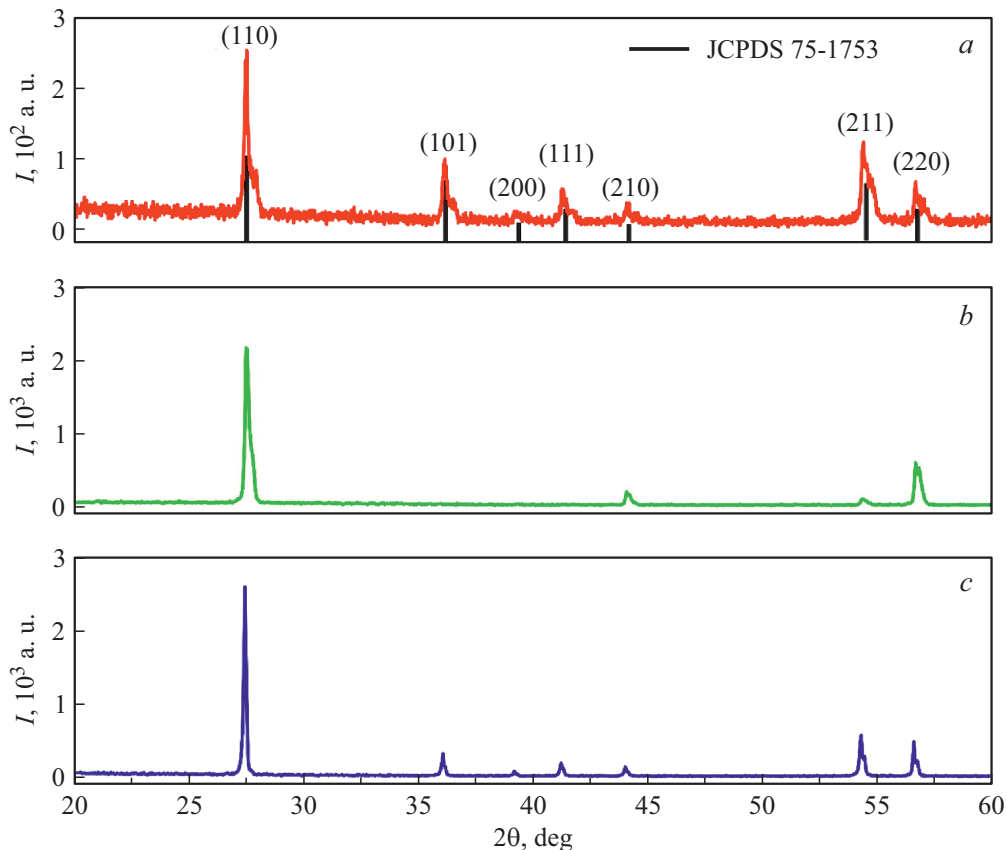


**Figure 2.** Diffraction patterns of the  $\text{TiO}_2$  samples obtained at  $T = 700$  (a),  $800$  (b) and  $900^\circ\text{C}$  (c).

Fig. 1, *a–c* presents SEM images of surfaces of the  $\text{TiO}_2$  samples obtained at  $T = 700, 800, 900^\circ\text{C}$ , respectively. The temperature range was chosen so as, on the one side, to exclude formation of titanium dioxide in the anatase modification that typically arises at  $T < 500^\circ\text{C}$ , and, on the other side, to exclude formation of titanium nitrides ( $T < 1000^\circ\text{C}$ ) [7]. In the case of a sample obtained at  $700^\circ\text{C}$  (Fig. 1, *a*), nanoscale (15–30 nm) crystallites form agglomerates 70–150 nm in size. At the temperature of  $800^\circ\text{C}$  (Fig. 1, *b*), there arise dendrite structures consisting of separate nanostructures 500–2000 nm in length and 100–200 nm in diameter; in contrast to the sample obtained

at  $700^\circ\text{C}$ , separate nanoscale granules are not visible in this case. This fact allows suggesting a hypothesis that the temperature increase to  $800^\circ\text{C}$  promotes texturing and coalescence of  $\text{TiO}_2$  nanogranules into nanoclusters, which, in its turn, results in anisotropic growth of nanocrystallites and formation of dendrite structures. As Fig. 1, *c* shows, further temperature increase leads to formation of close-packed nanostructures 100–300 nm in size.

The procedures for estimating separate crystallite sizes, as well as for determining structural parameters of crystal lattices of the  $\text{TiO}_2$  samples fabricated at different temperatures, involved XRD (Fig. 2). Based on the

literature data and data bases JCPDS (75-1753), ICDD PDF-2 (N 01-072-4819, 01-076-0317), it is possible to conclude that all the presented diffraction patterns relate to titanium dioxide with the tetragonal syngony of spatial group *P42/mnm* of the rutile structural modification [8–10]. The diffraction patterns differed from each other in both the numbers of reflection angles and intensities and half-widths of diffraction reflections, which evidences for different volumes of the formed oxides and different crystallite sizes and textures. Diffraction patterns of samples obtained at the temperatures of 700 and 900°C (Fig. 2, *a, c*) evidence for the polycrystalline structure of titanium oxide. However, in the case of the sample obtained at 800°C (Fig. 2, *b*) only two intense reflections are observed, which correspond to parallel crystallographic planes (110) and (220). This fact, on the one hand, evidences for the oxide textured character and, on the other hand, indicates the existence of preferable directions of the nanocrystallite growth, for instance, perpendicular to the [110] direction. Table 1 lists the calculated interplane distances in the lattice as compared with literature data.

Using the Debye–Scherrer equation

$$D = K\lambda/\beta \cos \theta \quad (1)$$

average sizes of nanocrystallites obtained at  $T = 700, 800$  and  $900^\circ\text{C}$  were estimated; they appeared to be 25.23, 30.31 and 47.11 nm, respectively (Table 2), which agrees qualitatively with the SEM results.

In formula (1),  $D$  is the crystallite average size,  $K$  is the Scherrer constant,  $\lambda$  is the X-ray wavelength,  $\beta$  is the reflection full width at half maximum (FWHM),  $\theta$  is the diffraction angle. The Scherrer constant was selected taking into account the crystal structure symmetry; in the case of tetragonal syngony, it is  $K = 0.88$  [11] in average. Structural parameters were calculated via the formula for the tetragonal syngony with spatial group *P42/mnm*:

$$\frac{1}{d^2} = \frac{h^2 + k^2}{a^2} + \frac{l^2}{c^2}, \quad (2)$$

where  $h, k, l$  are the Miller indices,  $d$  is the interplane distance,  $a$  and  $c$  are the lattice parameters.

**Table 1.** Crystal lattice interplane distances and relevant literature data for comparison

<i>hkl</i>	$d_{hkl}, \text{\AA}$					
	700°C	800°C	900°C	[8]	[9]	[10]
110	3.25	3.25	3.26	3.27	3.25	3.25
101	2.49	–	2.49	2.51	2.49	2.49
200	2.30	–	2.30	2.31	2.30	2.30
111	2.19	–	2.19	2.20	2.19	2.19
210	2.05	2.05	2.06	2.07	2.05	2.05
211	1.68	1.69	1.69	1.70	1.69	1.69
220	1.62	1.62	1.63	1.64	1.62	1.62

**Table 2.** Crystal lattice structural parameters and average parameters of crystallites

Sample TiO <sub>2</sub>	$V_{cell}, \text{\AA}^3$	$D, \text{nm}$	Lattice parameters	
			$a, \text{\AA}$	$c, \text{\AA}$
700°C	62.37	25.23	4.59	2.96
800°C	62.37	30.31	4.59	2.96
900°C	62.90	47.11	4.61	2.96
Data from [8]	63.88		4.63	2.98
Data from [9]	62.39		4.59	2.96
Data from [10]	62.39		4.59	2.96

The results of X-ray diffraction analysis (Table 1) exhibit qualitative agreement with literature data on the TiO<sub>2</sub>–rutile formation by different techniques. The calculations (Table 2) show that the increase in temperature gives rise to a tendency for growth of structural elements forming nanogranules and dendrites. An increase in sizes of the structural elements, as well as variations in intensities and numbers of the diffraction reflections, suggests formation of nanooxides of different shapes: nanocubes, nanorods and nanoplatelets. This fact explains the observed morphology of the SEM structures shaped as agglomerates of nanograins for the sample obtained at  $T = 700^\circ\text{C}$  and nanoplatelets for the sample obtained at  $T = 900^\circ\text{C}$ . At the same time, the absence of a distinguishable signal from structural elements in the dendrite–structure samples ( $T = 800^\circ\text{C}$ ) suggests their oriented growth along parallel planes, which allows nanorods to get crosslinked with minimal surface defects.

Thus, this paper presents a simple and fast technique for forming TiO<sub>2</sub>–based nanostructures of different morphologies, which is confirmed by complementary studies based on SEM and XRD. Thermal oxidation of titanium foil  $50 \times 10 \times 0.08 \text{ mm}$  in size in an oxygen–containing medium with partial pressure  $P_{\text{O}_2} = 100 \text{ mbar}$  in three temperature modes ( $T = 700, 800, 900^\circ\text{C}$ ) with exposure time  $t = 1.5 \text{ min}$  results in formation of titanium dioxide structured as rutile. We assume that the nanostructure formation mechanism has different characters in different temperature modes, which provides nanostructures of different morphologies, sizes and volumes. For instance, at  $700^\circ\text{C}$  polycrystalline nanoscale agglomerates 70–150 nm in size get formed from TiO<sub>2</sub> nanograins 15–30 nm in size, while at  $800^\circ\text{C}$  a dendrite surface gets formed whose characteristic sizes are 500–2000 nm in length and 100–200 nm in diameter. At  $900^\circ\text{C}$ , nanostructures containing of larger structural elements 47 nm in size are formed. The proposed technique of titanium thermal oxidation in an oxygen–containing gaseous phase and of controlling the obtained nanostructure morphologies is promising for fast and controllable obtaining oxide nanomaterials over a vast surface, which opens certain opportunities for sensorics and catalysis.

## Acknowledgements

The authors are grateful for the administration of CCU „Nanostructures Physics and Technology“ for X–ray diffraction studies.

## Financial support

The study was supported by the Russian Foundation for Basic Research (project № 20-52-04015), Belarussian Foundation for Basic Research (project № Ф21PM-054), and also by the RF Ministry of Science and Higher Education (State Assignment for Research Activity № FENW-2022-0001).

## Conflict of interests

The authors declare that they have no conflict of interests.

## References

- [1] C. Wang, D. Astruc, *Chem. Soc. Rev.*, **43** (20), 7188 (2014). DOI: 10.1039/C4CS00145A
- [2] G. Žerjav, M. Roškarič, J. Zavašnik, J. Kovač, A. Pintar, *Appl. Sur. Sci.*, **579**, 152196 (2022). DOI: 10.1016/j.apsusc.2021.152196
- [3] M. Murdoch, G.I.N. Waterhouse, M.A. Nadeem, J.B. Metson, M.A. Keane, R.F. Howe, J. Llorca, H. Idriss, *Nature Chem.*, **3**, 489 (2011). DOI: 10.1038/nchem.1048
- [4] D.A.H. Hanaor, C.C. Sorrell, *J. Mater. Sci.*, **46** (4), 855 (2011). DOI: 10.1007/s10853-010-5113-0
- [5] S.V. Bulyarskiy, G.G. Gusarov, D.A. Koiva, G.A. Rudakov, *Phys. Solid State*, **63**, 1611 (2021). DOI 10.1134/S1063783421100061.
- [6] A.A. Sivkov, D.Yu. Gerasimov, D.S. Nikitin, *Tech. Phys. Lett.*, **43**, 16 (2017). DOI: 10.1134/S1063785016120105.
- [7] T. Krekeler, S.S. Rout, G.V. Krishnamurthy, M. Störmer, M. Arya, A. Ganguly, D.S. Sutherland, S.I. Bozhevolnyi, M. Ritter, K. Pedersen, A.Yu. Petrov, M. Eich, M. Chirumamilla, *Adv. Opt. Mater.*, **9** (16), 2100323 (2021). DOI: 10.1002/adom.202100323
- [8] M. Okrusch, R. Hock, U. Schüssler, A. Brummer, M. Baier, H. Theisinger, *Am. Mineral.*, **88** (7), 986 (2003). DOI: 10.2138/am-2003-0706
- [9] X. Bokhimi, A. Morales, F. Pedraza, *J. Solid State Chem.*, **169** (2), 176 (2002). DOI: 10.1016/S0022-4596(02)00046-4
- [10] K. Sugiyama, Y. Takéuchi, *Z. Kristallogr. — Cryst. Mater.*, **194** (1-4), 305 (1991). DOI: 10.1524/zkri.1991.194.14.305
- [11] J.I. Langford, A.J.C. Wilson, *J. Appl. Cryst.*, **11**, 102 (1978). DOI: 0.1107/S0021889878012844